AMT 26 Ship-Borne C-band NRCS measurements.

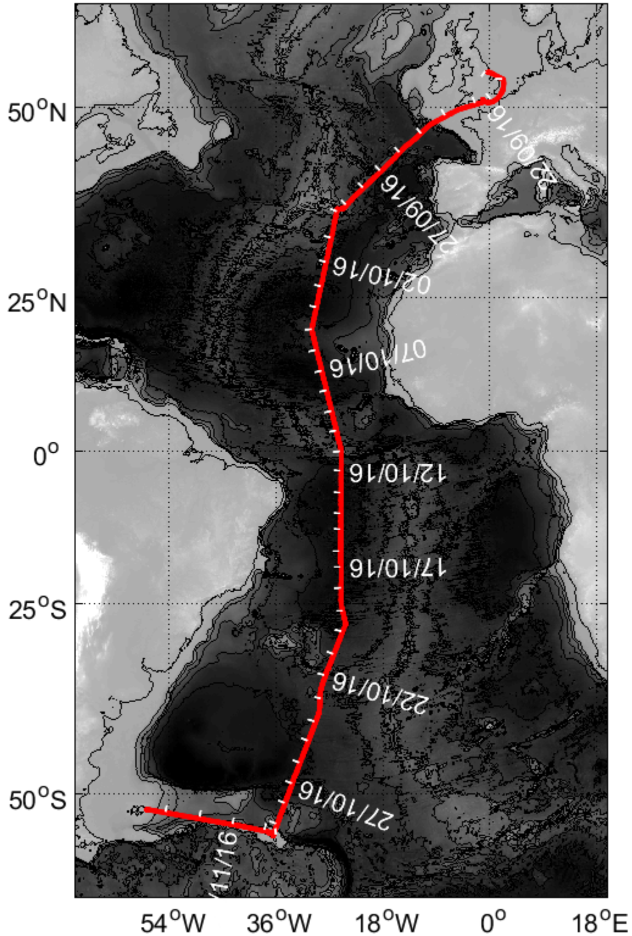

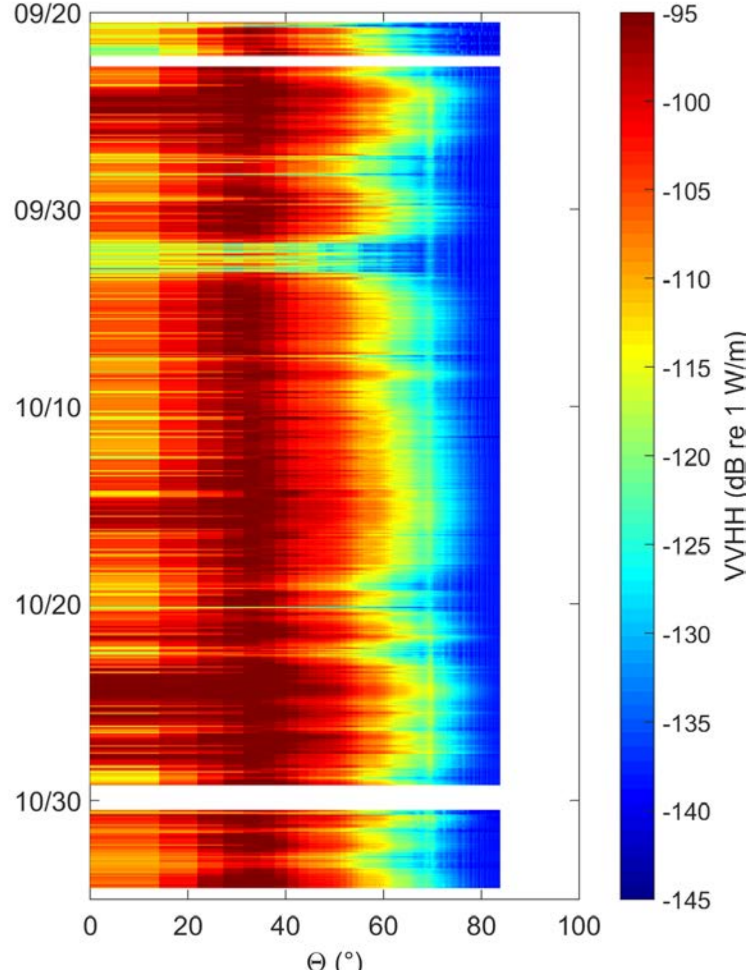

<u>L. Marié</u>, A. Mouche, B. Chapron, F. Nouguier, P. Sutherland, W. Wimmer, Y. Zhao.

AMT4SentinelFRM Meeting, Plymouth, 06/2017.

The Sentinel 1 A/B Synthetic Aperture Radars (1)

S1A, 2016/09/23, 06:33 TU, VV, ® ESA

<u>Radar Scatterometry:</u>

The observable is the capacity of the sea surface to reflect the radar signal at C-band (λ~6 cm) towards the satellite.

The « normalized return cross section » (NRCS) $\sigma 0$ is related to the power transmitted and received by the instrument by the « radar equation » (Ulaby 1982)

$$P_j^r = \frac{\lambda^2}{4\pi} \times P_i^t \times G_j^A \times \int G_i^t(\theta,\varphi) \times G_j^r(\theta,\varphi) \times \frac{\sigma_{ij}^0(\theta,\varphi)}{(4\pi R^2)^2} \times dA$$

+: goes through clouds, no or little atmospheric effect, not dependent on external illumination, very high resolution.

- : $\sigma 0$ it is, and whatever geophysical variable we may be interested in must be retrieved from it.

The Sentinel 1 A/B Synthetic Aperture Radars (2)

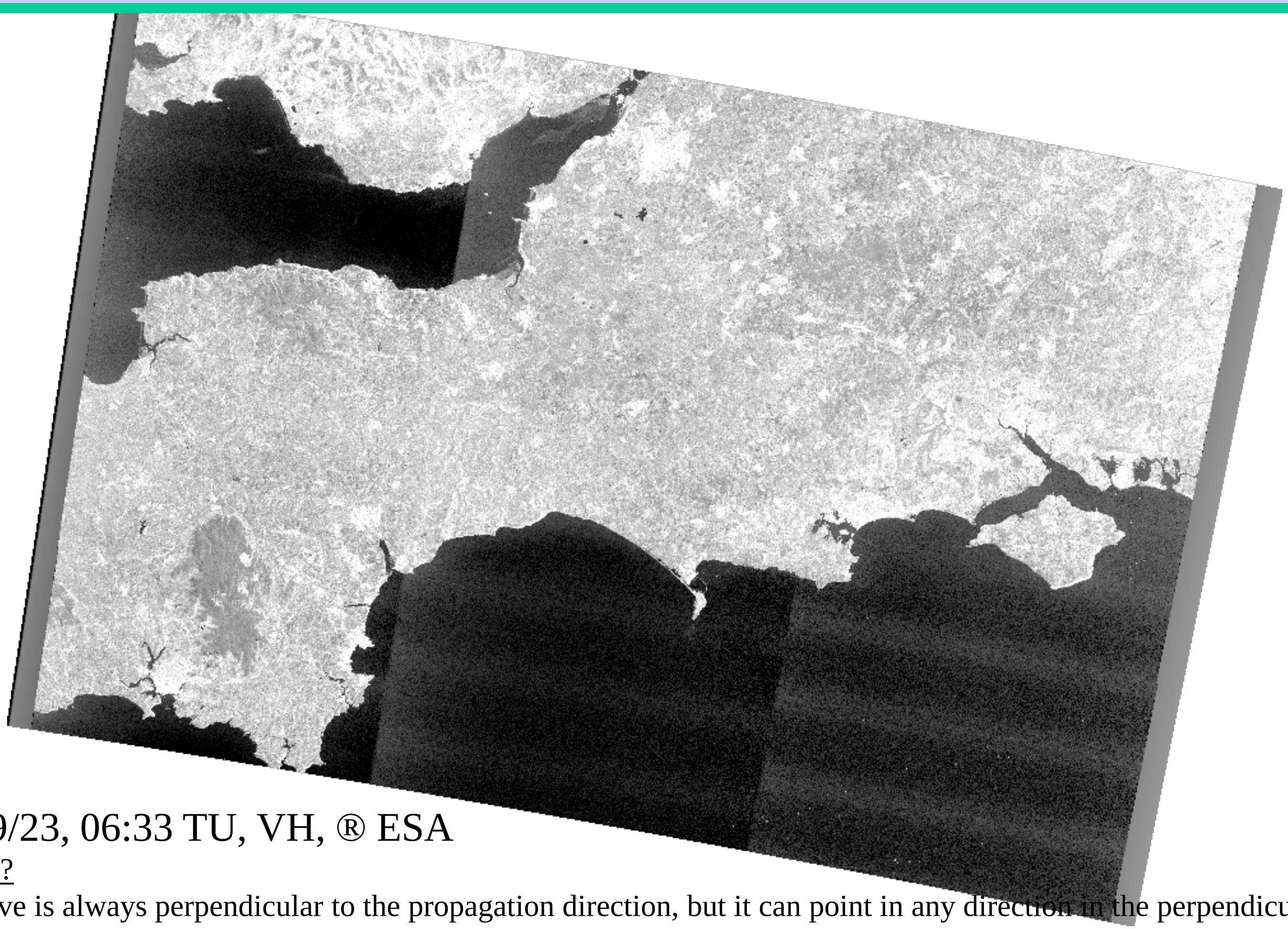

S1A, 2016/09/23, 06:33 TU, VH, ® ESA

Why « Polarimetric »?

The **E**-field in the wave is always perpendicular to the propagation direction, but it can point in any direction in the perpendicular plane.
In particular, it can be transmitted in a vertical plane or parallel to the sea surface (« V » / « H » polarizations respectively)
When V-polarized waves hit the sea surface, most of the energy returns in V-pol, but some is converted to H-pol. There are VV and VH NRCSs.
And conversely, there are HH and HV NRCSs.
The synthetic aperture radar onboard S-1A and S-1B can transmit either polarizations (but only one at a time), and receive in both polarizations simultaneously.
Some things show up better in VV than in HH, or in the cross-polarized signals that in the co-polarized ones.
One major challenge here is that the VH and HV signals are a lot harder to measure than the VV and HH ones, which are expected to be a lot stronger. So a lot less is known about the behaviour of these signals. But there are strong incentives to use them in future instruments.

The Sentinel 1 A/B Synthetic Aperture Radars (3)

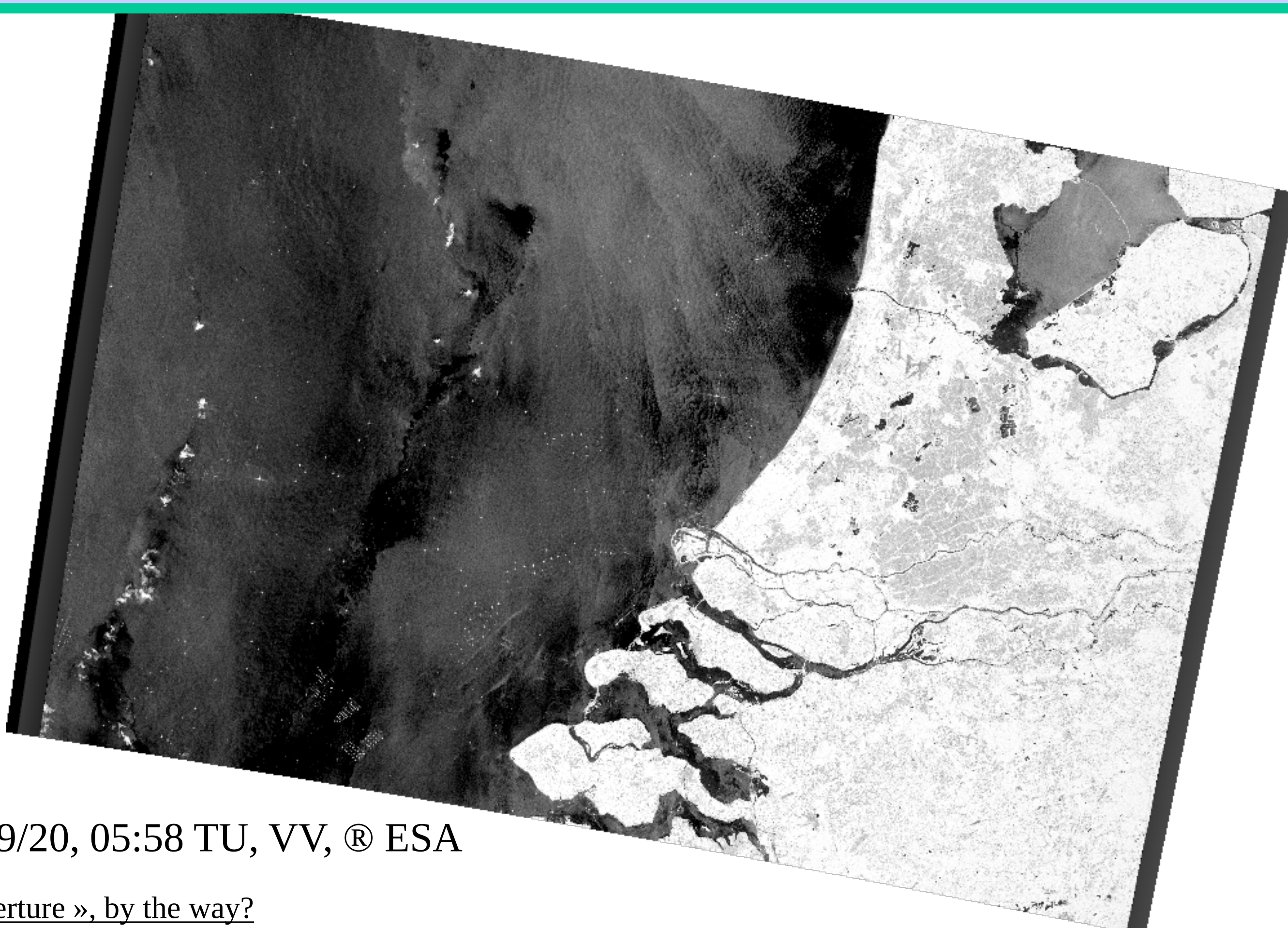

S1A, 2016/09/20, 05:58 TU, VV, ® ESA

<u>Why « Synthetic Aperture », by the way?</u>

The angular resolution of a teledetection system which measures waves in the far-field is proportional to the ratio of the working wavelength over the aperture size of the detector.

Optical instruments use light with wavelength in the micron range, with apertures in the decimeter range, and achieve resolutions in the hundred meters range.

Achieving a similar ground resolution with a wavelength 100000 larger would thus require an impractically large antenna!

« Real Aperture » scatterometers use physical antennas several meters wide, and provide output with a resolution of several tens of kilometers.

« Synthetic Aperture Radars » use a smarter approach: signals transmitted at different instants along the satellite flight path are phase-coherently combined, to produce the same result as would have been achieved with an antenna several kilometers long.

In-situ measurements for The Sentinel 1 A/B SARs Cal/Val?

SAR Cal/Val is usually (and very well) performed by comparison with in-flight similar instruments.

Relationships with ground observables (wind speed, sea state) are established by comparing measurements obtained from space with moored instruments or other space-borne instruments (scatterometers).

No (affordable) equivalent of the ISAR or of Trioses or other deployable spectrometers existed.

Still, many aspects of the radiation-sea surface interactions are not yet satisfactorily understood (cross-pol signals, impact of breaking, high-wind behaviour…).

⇒ development at IFREMER of a field-deployable range-resolved polarimetric C-band radar.

⇒ first « live » deployment during AMT 26, along with a CCTV camera to take images of the sea surface.

⇒ thanks to W. Wimmer, we also have high-quality wind data.

⇒ thanks to W. Wimmer and F. Nencioli, the instrument actually came back from the Falklands...

Instrument onboard the JCR

The ship-borne C-band radar: working principle

50 times per second, the radar transmits C-band (5.2 GHz $\rightarrow$ 5.4 GHz) chirped signals in V-pol and H-pol. The two signals are slightly offset in frequency (0.02 GHz).

The receiving horn antenna has 2 ports, one for the V-pol and one for the H-pol.

On both ports, the signal first passes through a Low-Noise amplifier, then a general-purpose C-band amplifier, then a splitter to be routed to a total of 4 detection channels.

In each detection channel, the signal is demodulated by one of the transmit signals, and the baseband signal is digitized at 51200 Hz using a 24-bit Sigma-Delta digitizer.

Demodulating with the V transmit signal the signal received by the H port of the receive antenna gives access to the VH backscattered amplitude, for instance.

Each segment of the received baseband signal is then Fourier-transformed to give a range-resolved record of the backscattering amplitude in the 4 co- and cross-polarizations.

Schematic

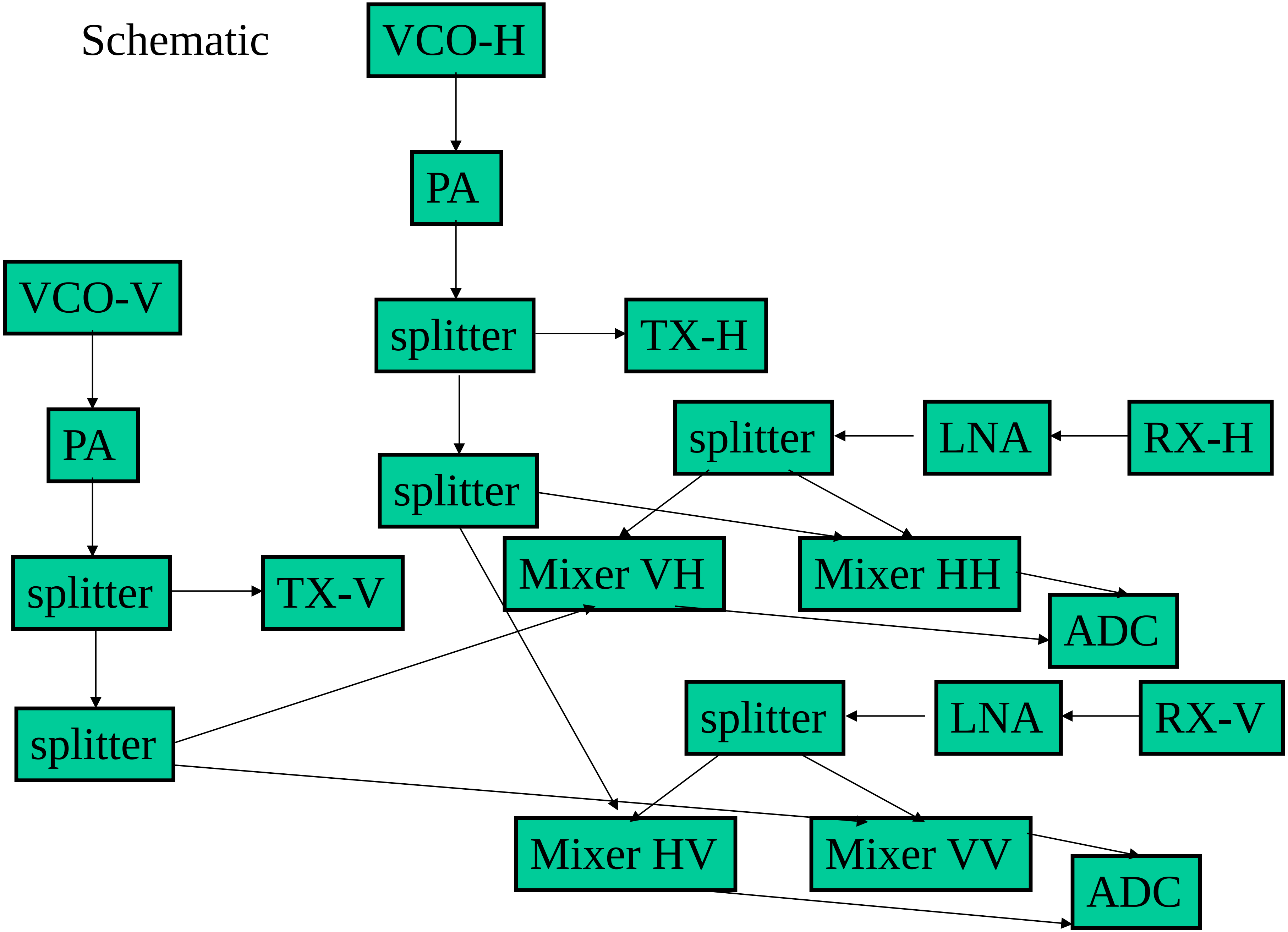

VCO-H
PA
splitter
TX-H
splitter
VCO-V
PA
splitter
TX-V
splitter
splitter
LNA
RX-H
Mixer VH
Mixer HH
ADC
splitter
LNA
RX-V
Mixer HV
Mixer VV
ADC

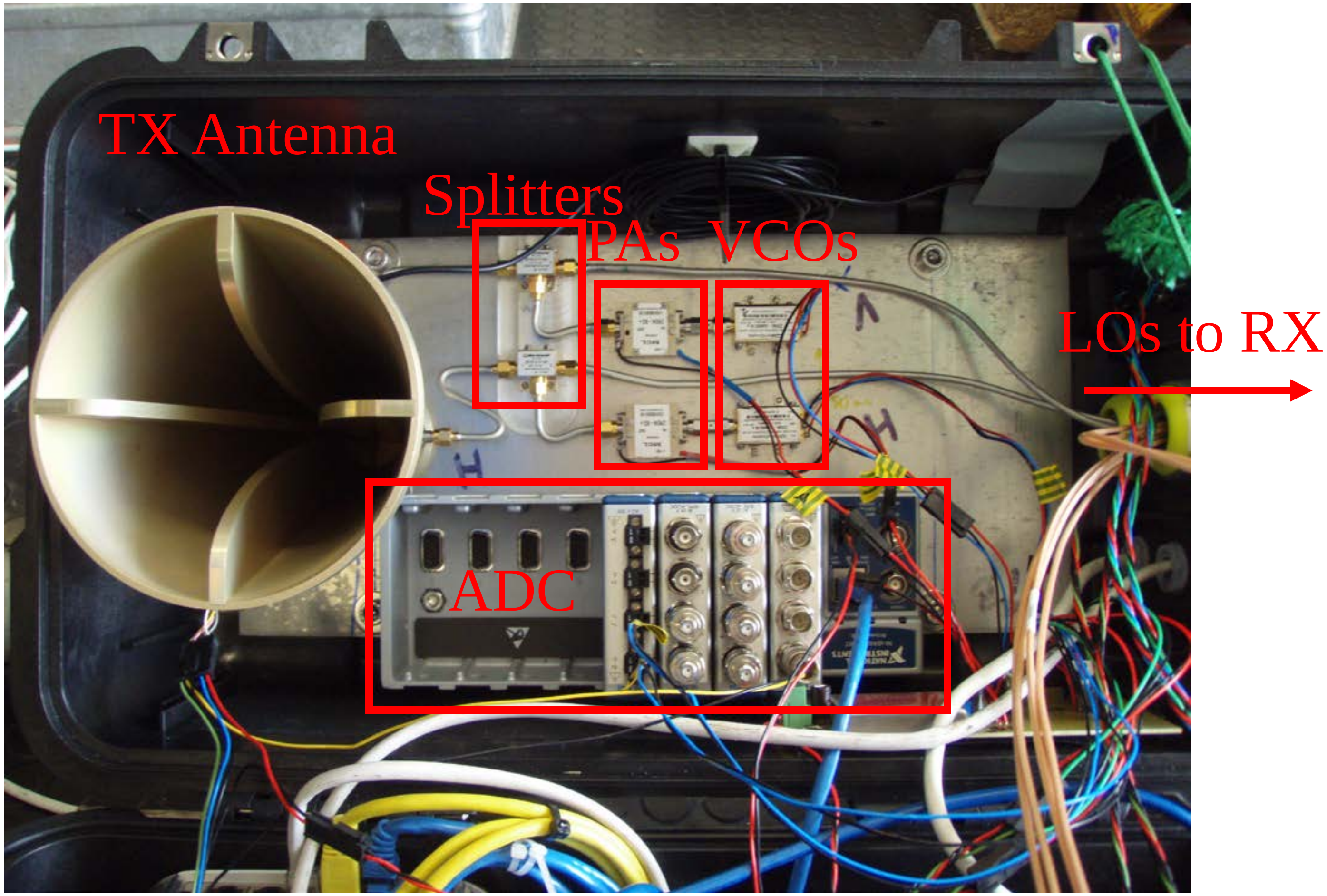

+ MTI-G Motion package
+ input ports for GPS and Gill MetPack II sensor

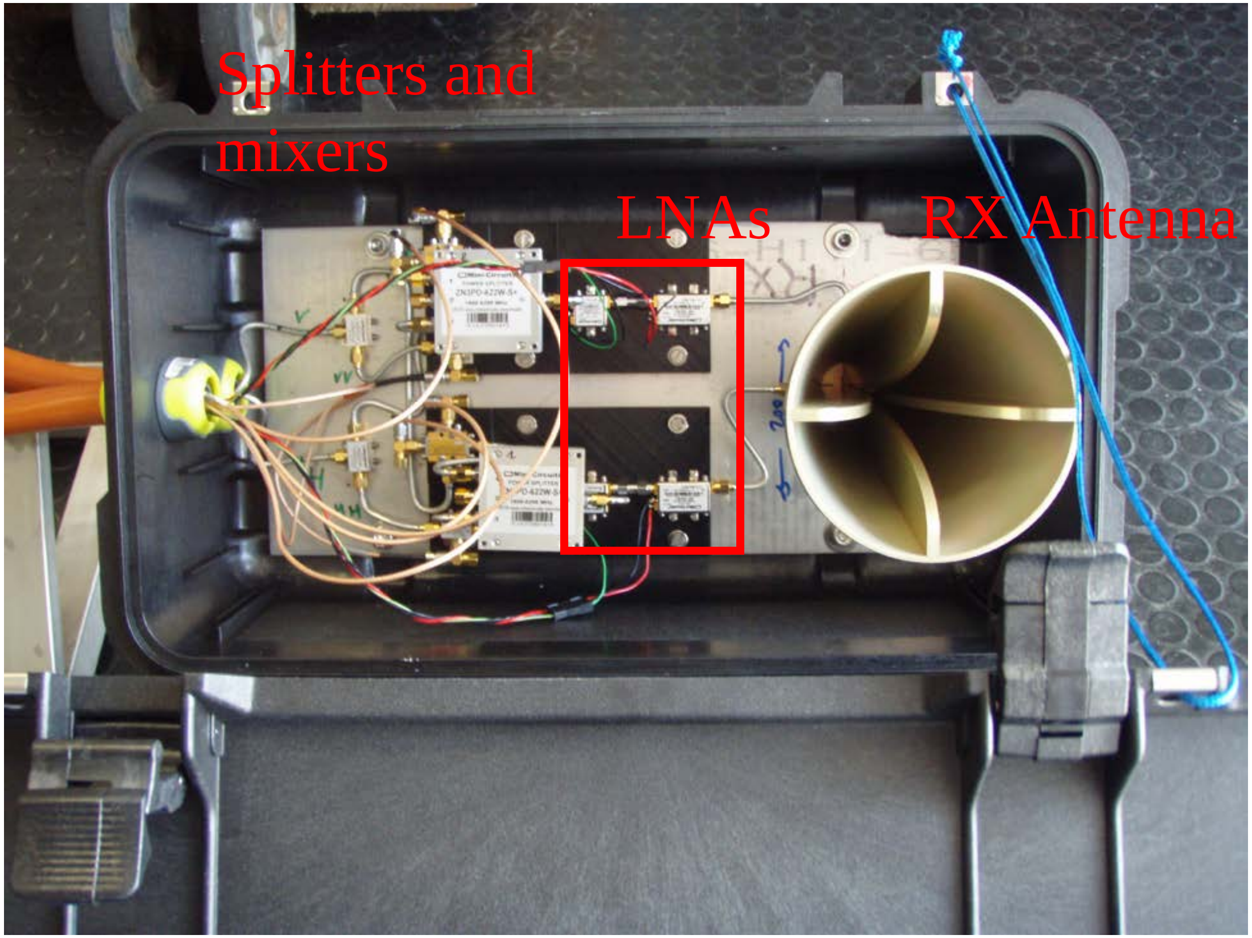

Splitters and mixers
LNAs
RX Antenna

AMT 2016 Track

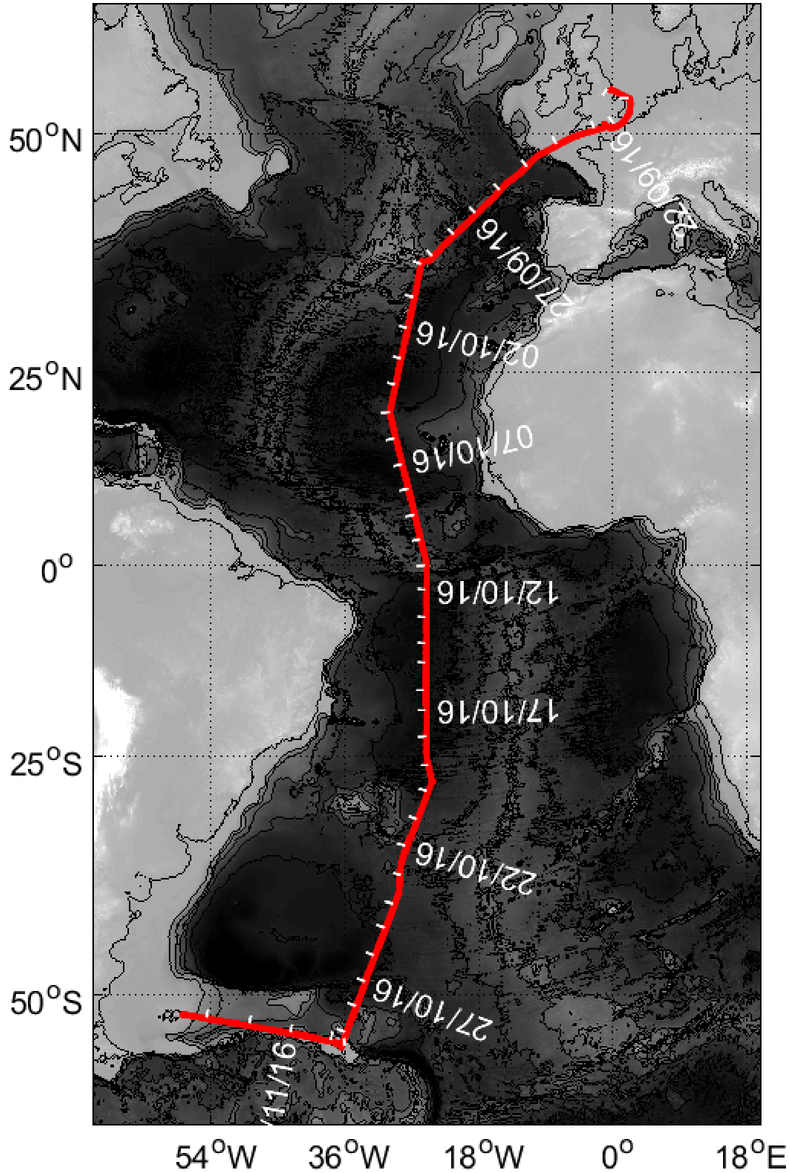

Every 20 minutes, 4 minutes acquisition at
50 pings-per-second.

Together with 2 Hz B/W images (daytime only).

⇒ 2267 valid data segments.

⇒ 947 invalid data segments (no signal?).

⇒ firmware bug:
VV and HH mix-up, only VV+i HH was stored
(VH and HV are OK).

Sample data (1)

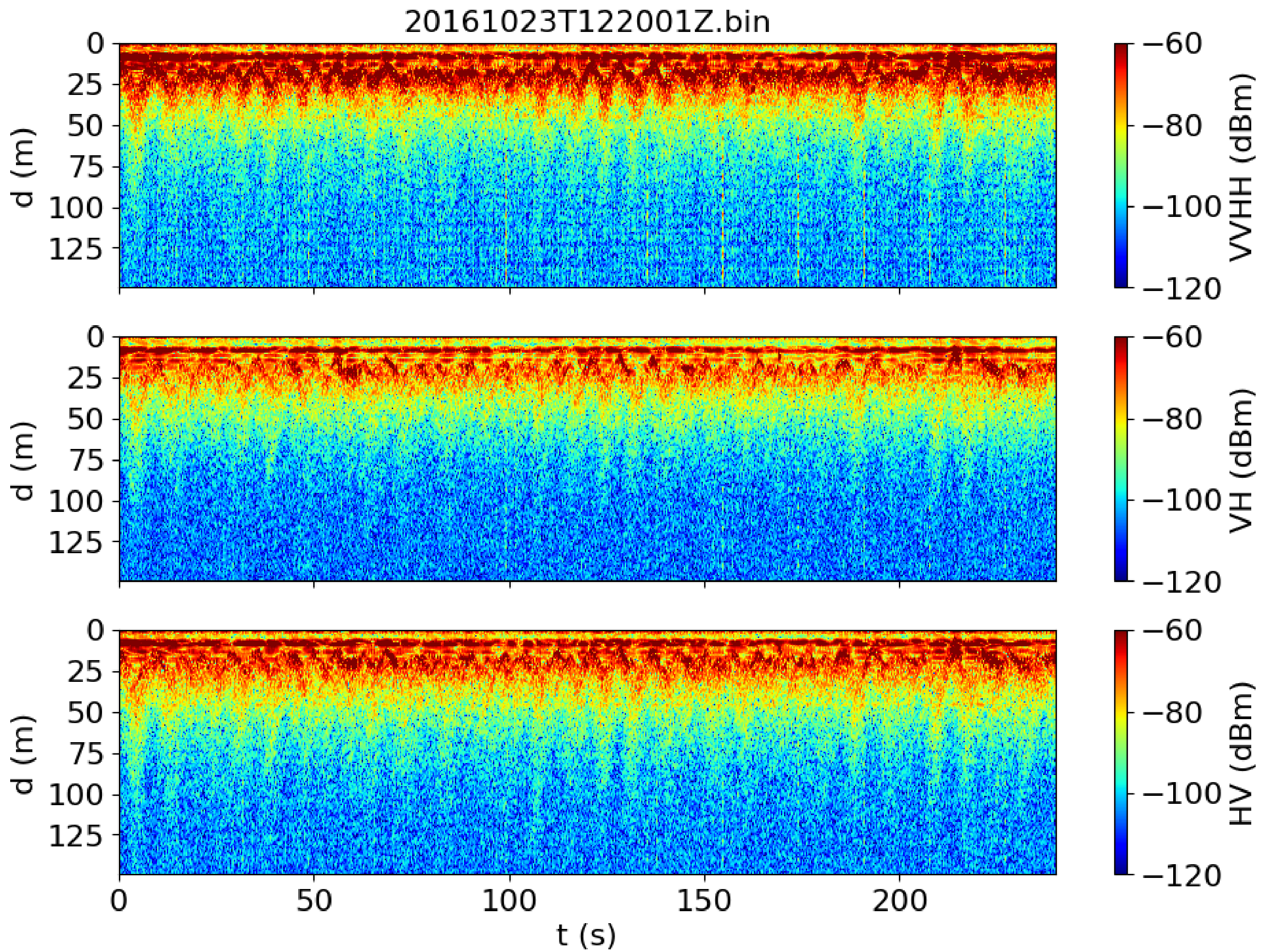

Sample data (2)

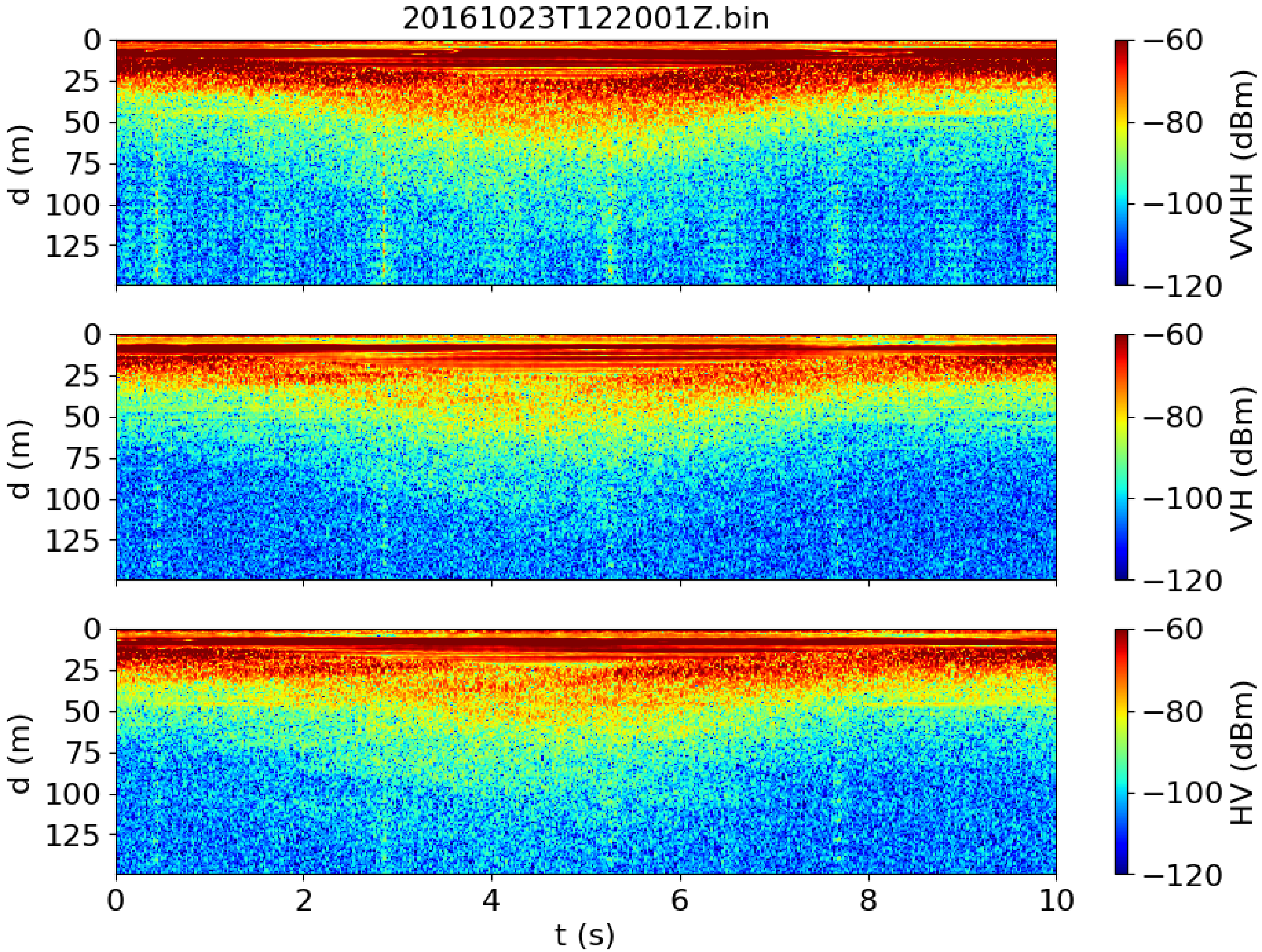

Sample data (3)

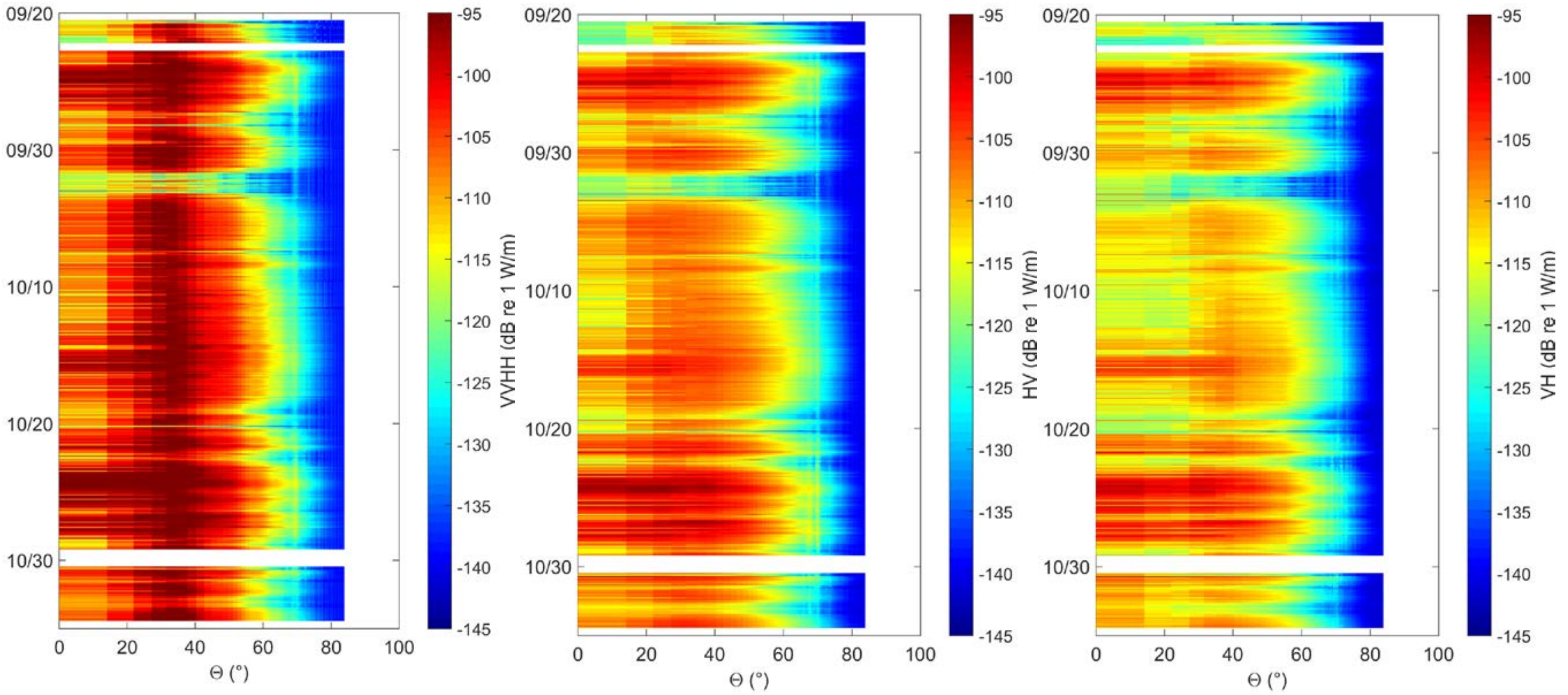

These are raw receive power observations.
Not yet σ0…

Going to geophysical data (1)

The radar cross-section σ_0 for a distributed target is defined by the « Radar equation » (Ulaby 1982):

$$P_j^r = \frac{\lambda^2}{4\pi} \times P_i^t \times G_j^A \times \int G_i^t(\theta,\varphi) \times G_j^r(\theta,\varphi) \times \frac{\sigma_{ij}^0(\theta,\varphi)}{(4\pi R^2)^2} \times dA$$

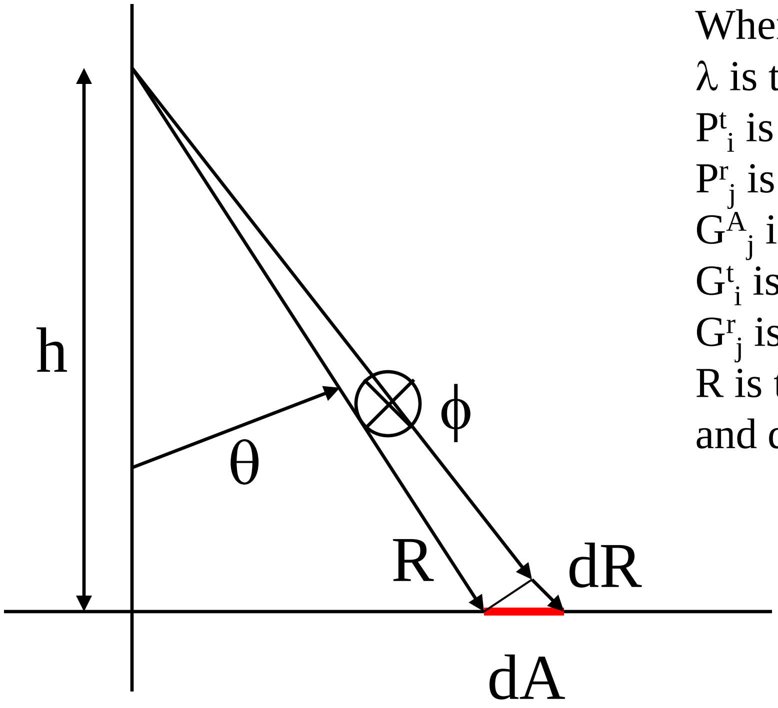

Where:
λ is the carrier wavelength,
P^t_i is the transmitted power in polarization i,
P^r_j is the received power in polarization j,
G^A_j is the reception chain gain in polarization j,
G^t_i is the gain of the transmission antenna in polarization i,
G^r_j is the gain of the reception antenna in polarization j,
R is the distance to the imaged patch,
and dA is the image patch area increment.

$$\begin{aligned} dA &= h^2 \times \frac{\sin(\theta)}{\cos^3(\theta)} \times d\phi \times d\theta \\ &= R^2 \times \tan(\theta) \times d\phi \times d\theta \\ &= R \times dR \times d\phi \end{aligned}$$

Going to geophysical data (2)

So we have :

$$\frac{(4\pi)^3}{\lambda^2}\frac{P_j^r}{G_j^A P_i^t} = \int G_i^t(\theta,\varphi)\times G_j^r(\theta,\varphi)\times\frac{\sigma_{ij}^0(\theta,\varphi)}{R^3}\times d\varphi\times dR$$

But we have range-resolved measurements, so (θ is now a function of R, and P^r is in W/m):

$$\int G_i^t(\theta,\varphi)\times G_j^r(\theta,\varphi)\times\sigma_{ij}^0(\theta,\varphi)\times d\varphi = \frac{(4\pi)^3}{\lambda^2 G_j^A P_i^t}R^3 P_j^r(R)$$

And then a reasonable form for the antenna gains is (they are all very similar):

$$G_i^t(\theta,\varphi) = 18.80\times\frac{1}{2}^{\frac{\varphi^2}{0.1474}}\times\frac{1}{2}^{\frac{(\theta-\pi/4)^2}{0.1474}}$$

So we get to:

$$18.8^2\times\frac{1}{2}^{\frac{2(a\cos(h/R)-\pi/4)^2}{0.1474}}\times\int\frac{1}{2}^{\frac{2\varphi^2}{0.1474}}\times\sigma_{ij}^0(\theta,\varphi)\times d\varphi = \frac{(4\pi)^3}{\lambda^2 G_j^A P_i^t}R^3 P_j^r(R)$$

But then σ_0 varies slowly with ϕ, so we can take σ_0 out of the integral, to get:

$$\sigma_{ij}^0(\theta,\varphi)\times 18.8^2\times\frac{1}{2}^{\frac{2(a\cos(h/R)-\pi/4)^2}{0.1474}}\times\int\frac{1}{2}^{\frac{2\varphi^2}{0.1474}}d\varphi = \frac{(4\pi)^3}{\lambda^2 G_j^A P_i^t}R^3 P_j^r(R)$$

$$\sigma_{ij}^0(\theta,\varphi)\times 18.8^2\times\frac{1}{2}^{\frac{2(a\cos(h/R)-\pi/4)^2}{0.1474}}\times\sqrt{\frac{0.1474\pi}{2\log(2)}} = \frac{(4\pi)^3}{\lambda^2 G_j^A P_i^t}R^3 P_j^r(R)$$

Going to geophysical data (3)

So we have :

$$\sigma_{ij}^0(\theta,\varphi) = \frac{(4\pi)^3}{\lambda^2 G_j^A P_i^t} \sqrt{\frac{2\log(2)}{0.1474\pi}} \frac{1}{18.8^2} 2^{\frac{2(a\cos(h/R)-\pi/4)^2}{0.1474}} R^3 P_j^r(R)$$

And we prefer to work with dB's, so:

$$\sigma_{ij}^0(\theta,\varphi) = 10\log_{10}\left(\sqrt{\frac{2\log(2)}{0.1474\pi}}\frac{(4\pi)^3}{18.8^2}\right) + 10\log_{10}\left(2^{\frac{2(a\cos(h/R)-\pi/4)^2}{0.1474}}\right) + 10\log_{10}\left(\frac{R^3 P_j^r(R)}{\lambda^2 P_i^t G_j^A}\right)$$

$$= 9.9 + 10\times\frac{2\log 2}{0.1474\log 10}\times(a\cos(h/R)-\pi/4)^2 + 30\log_{10} R + 10\log_{10}\left(\frac{P_j^r(R)}{\lambda^2 P_i^t G_j^A}\right)$$

We know 10 log10(Pt) $\in$[16.5 dBm; 19.5 dBm]
We know 10 log10(G^A) $\in$[24 dB; 25 dB] $\rightarrow$ 10 log10(Pt G^A) $\in$[40.5 dBm; 44.5 dBm]
We know λ=0.0566 m.
So, with R in m and Pr in W/m,

$$\sigma_{ij}^0(\theta,\varphi) = 10\log_{10} P_j^r(R) + 22.3 + 40.8\times(a\cos(h/R)-\pi/4)^2 + 30\log_{10} R$$

σ_0, at last… (1)

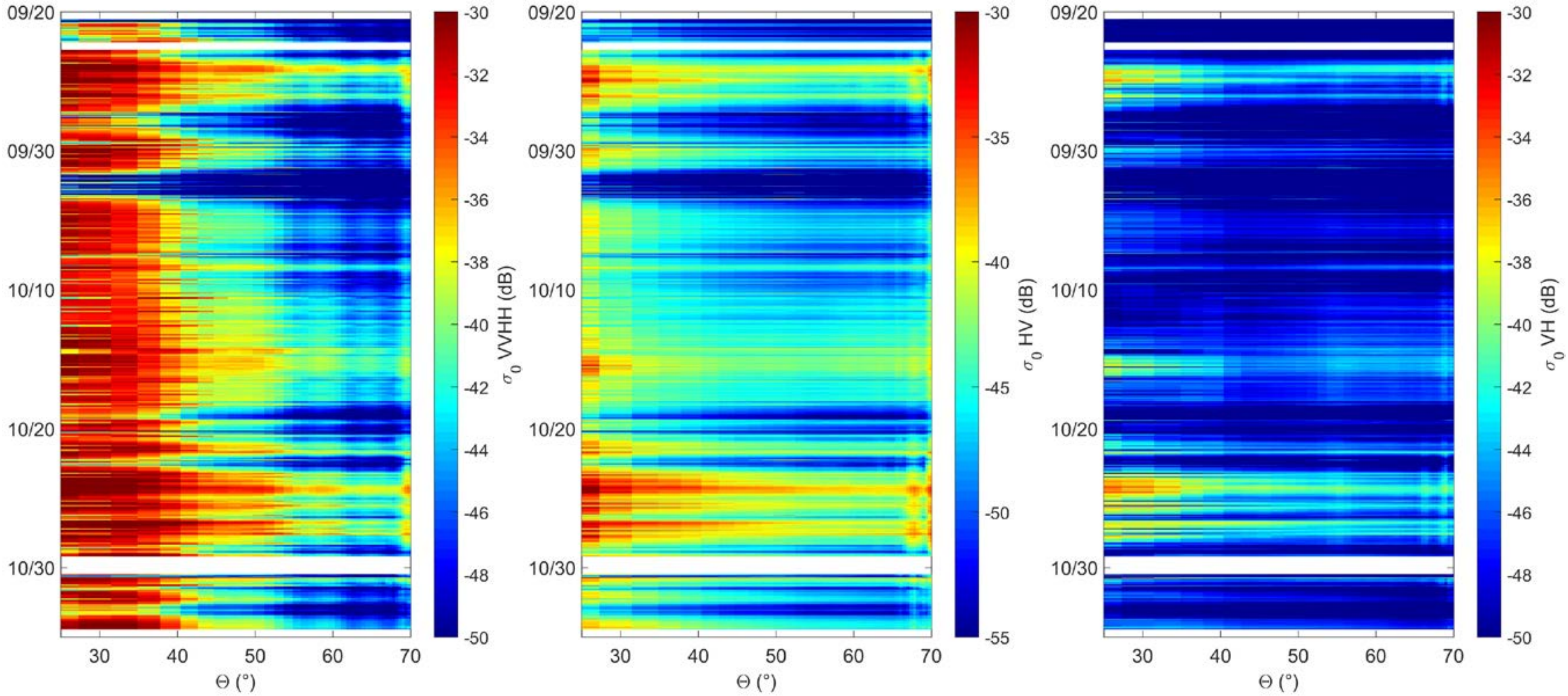

Wind-dependence of σ0 seems satisfactory.
Much weaker dependence of cross-pol σ0 with respect to incidence angle.
Probably some contamination of the HV channel by some VV signal.

σ_0, at last… (2)

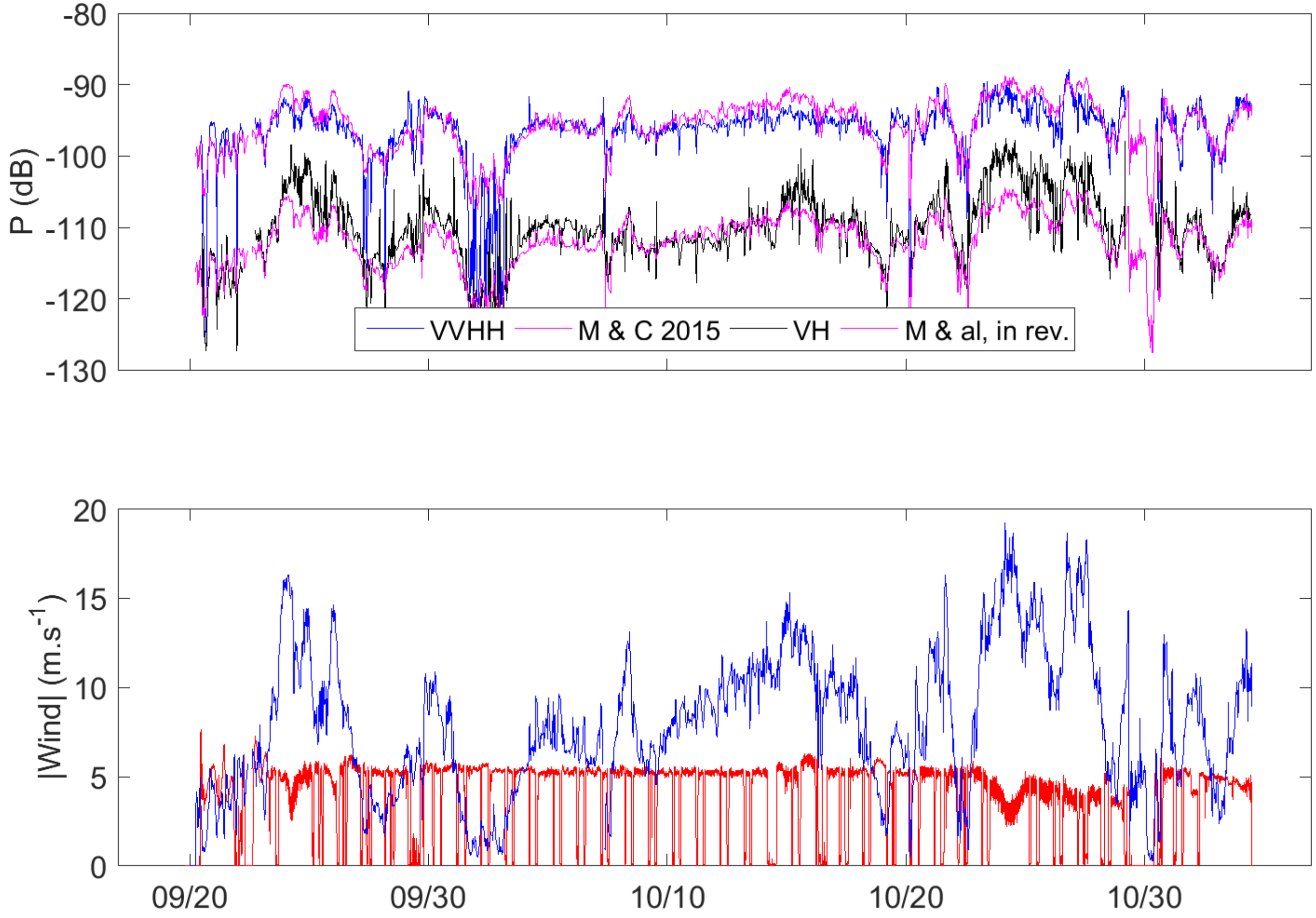

Wind-dependence of $\sigma 0$ seems satisfactory w.r.t. established models.
Some discrepancies for very high and very low wind speed (expected, interesting).

σ_0, at last… (3)

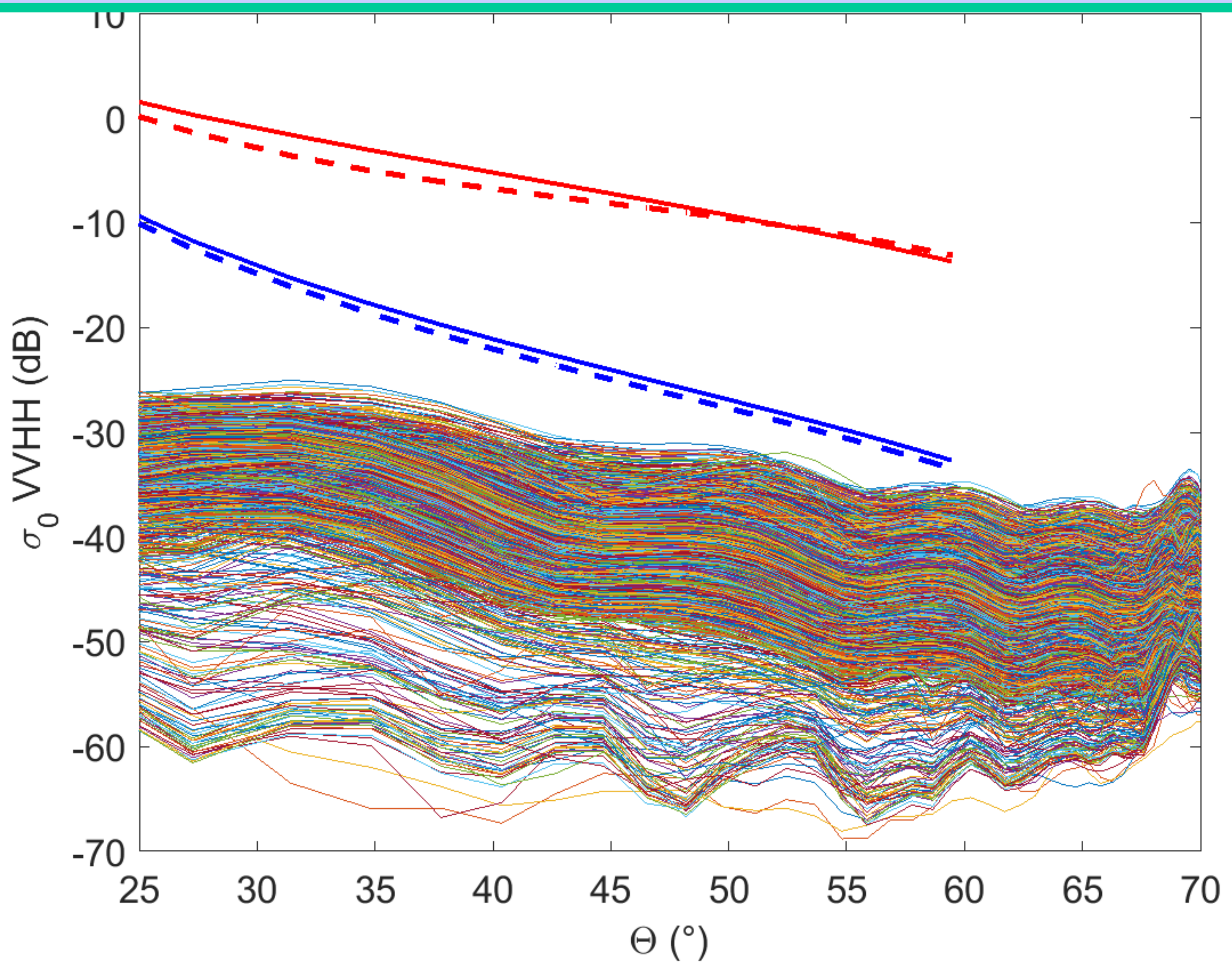

Still a few dBs off…

Dependence w.r.t. incidence angle seems almost reasonable.

σ_0, at last… (4)

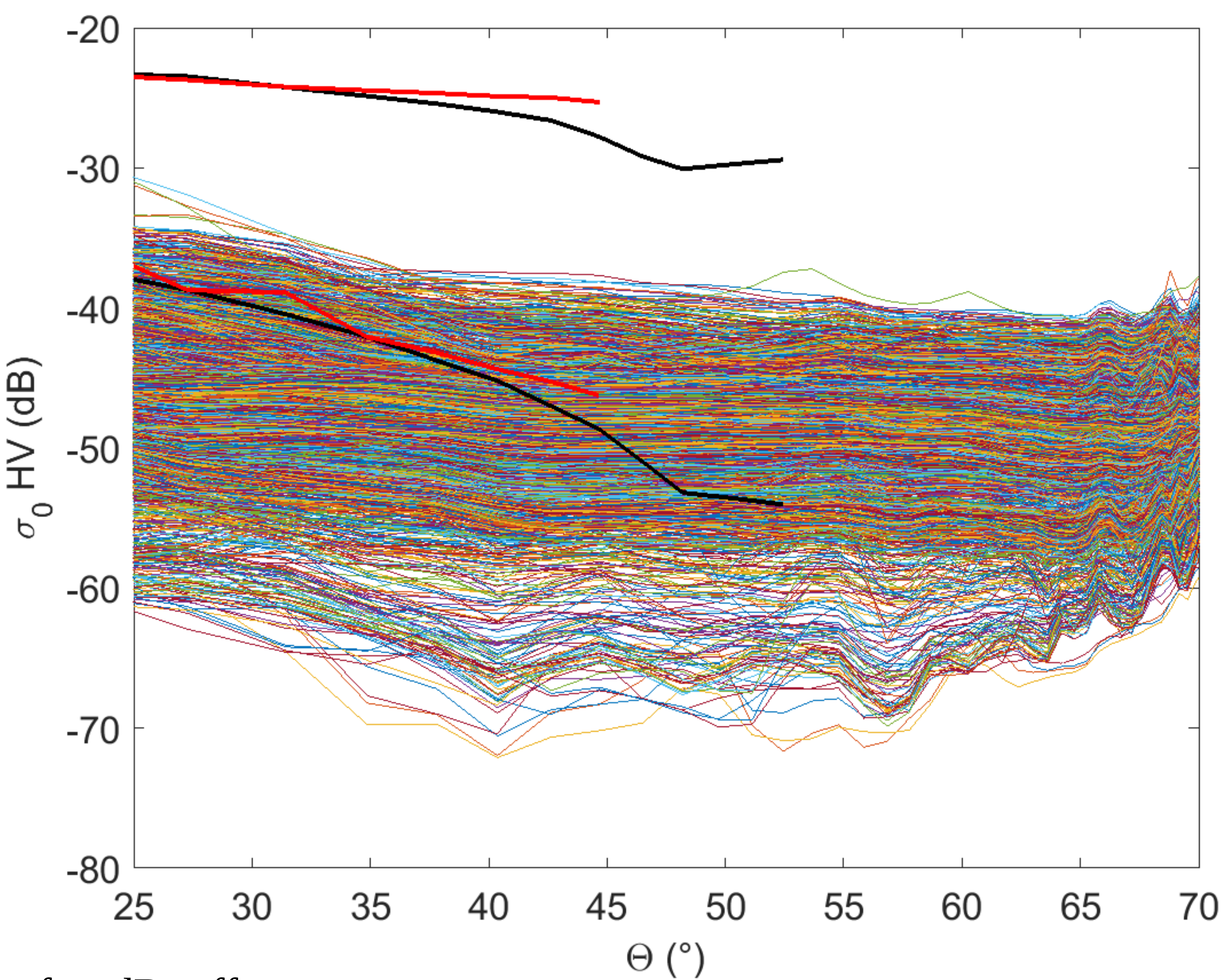

Still a few dBs off…

Incidence angle dependence is weak, as seems to be expected by Mouche et al, in rev.

Nothing in the data to confirm the dip in $\sigma 0$ predicted by the Hwang 2014 model.

σ_0, at last… (5)

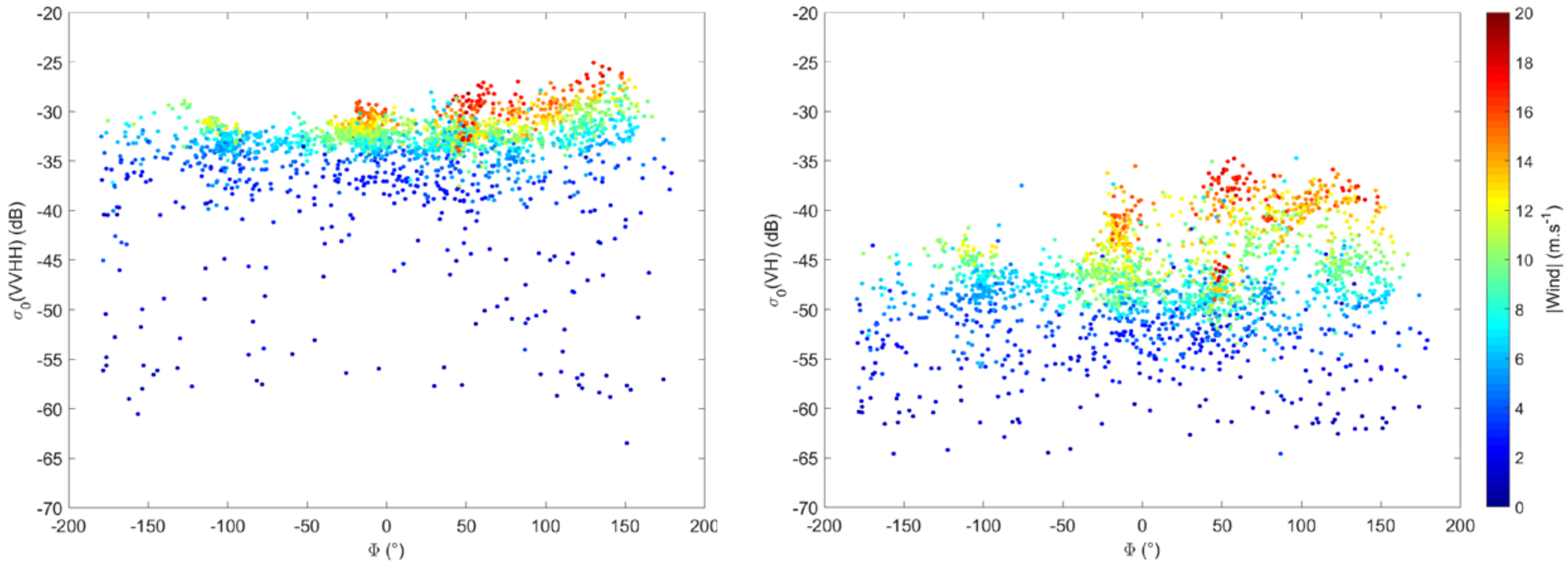

HV σ0 is weaker than VV+HH (expected).
Less saturation of HV than VV+HH at high winds (expected).
Dependence of σ0 w.r.t. up/downwind direction is weak for HV (Mouche et al, in rev.)

In South Georgia, theory works.

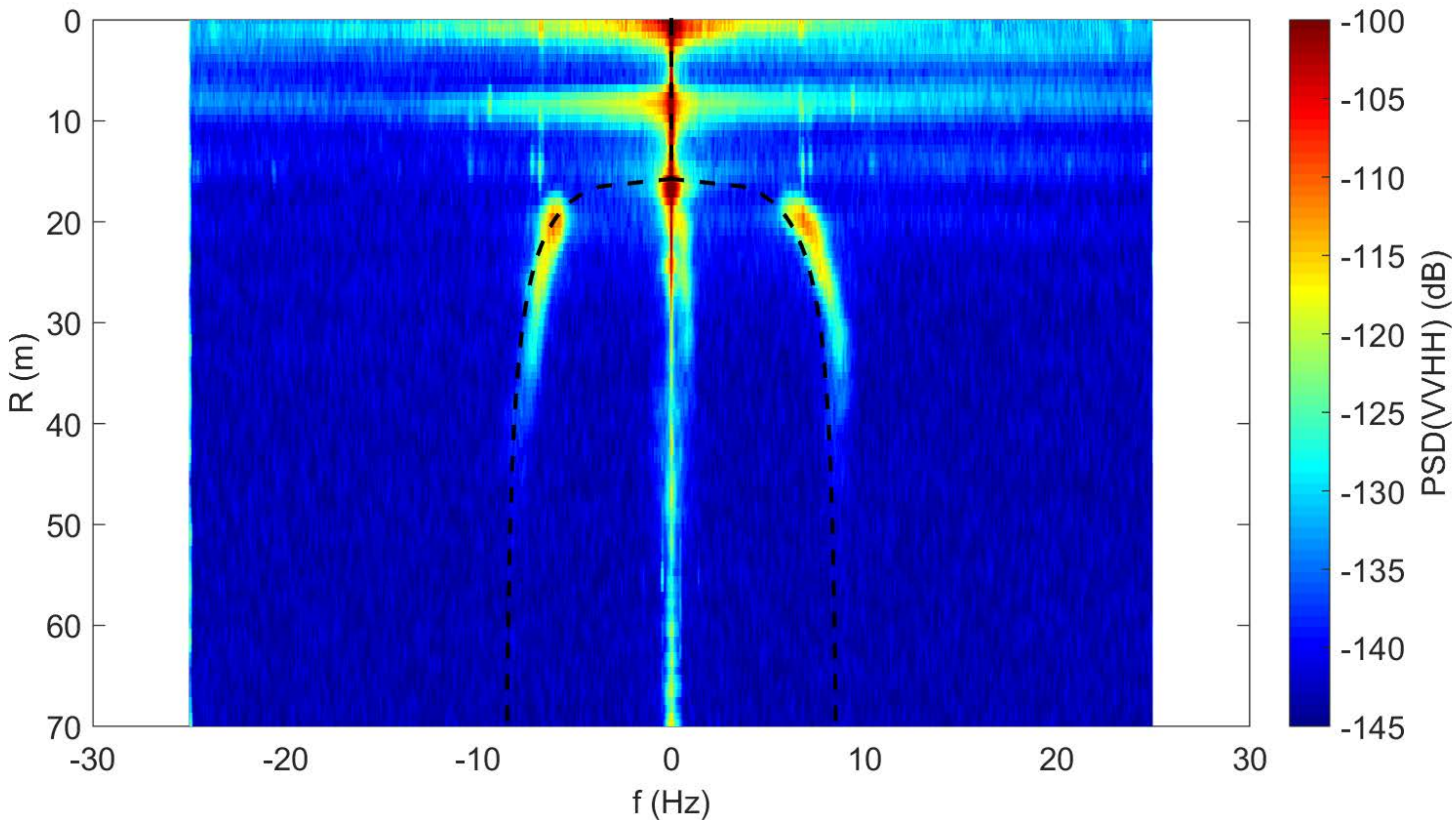

Doppler spectrum of radar return collects along the dispersion curves for gravity-capillary waves at the Bragg wavelength.
-> Seems to require very, very calm weather…

Perspectives:

Short-term:

⇒Refurbish the instrument for AMT 2017.
⇒Fix the firmware.
⇒Don’t touch anything else!!!!!!
⇒Make sure all S1 overpasses during the cruise are acquired (very few match-ups in 2016).

Mid-term:

⇒SI traceability??? (internal calibration channel + Standardized calibration targets?)
⇒Miniaturize, for easier deployments?

In South Georgia, theory works (2).

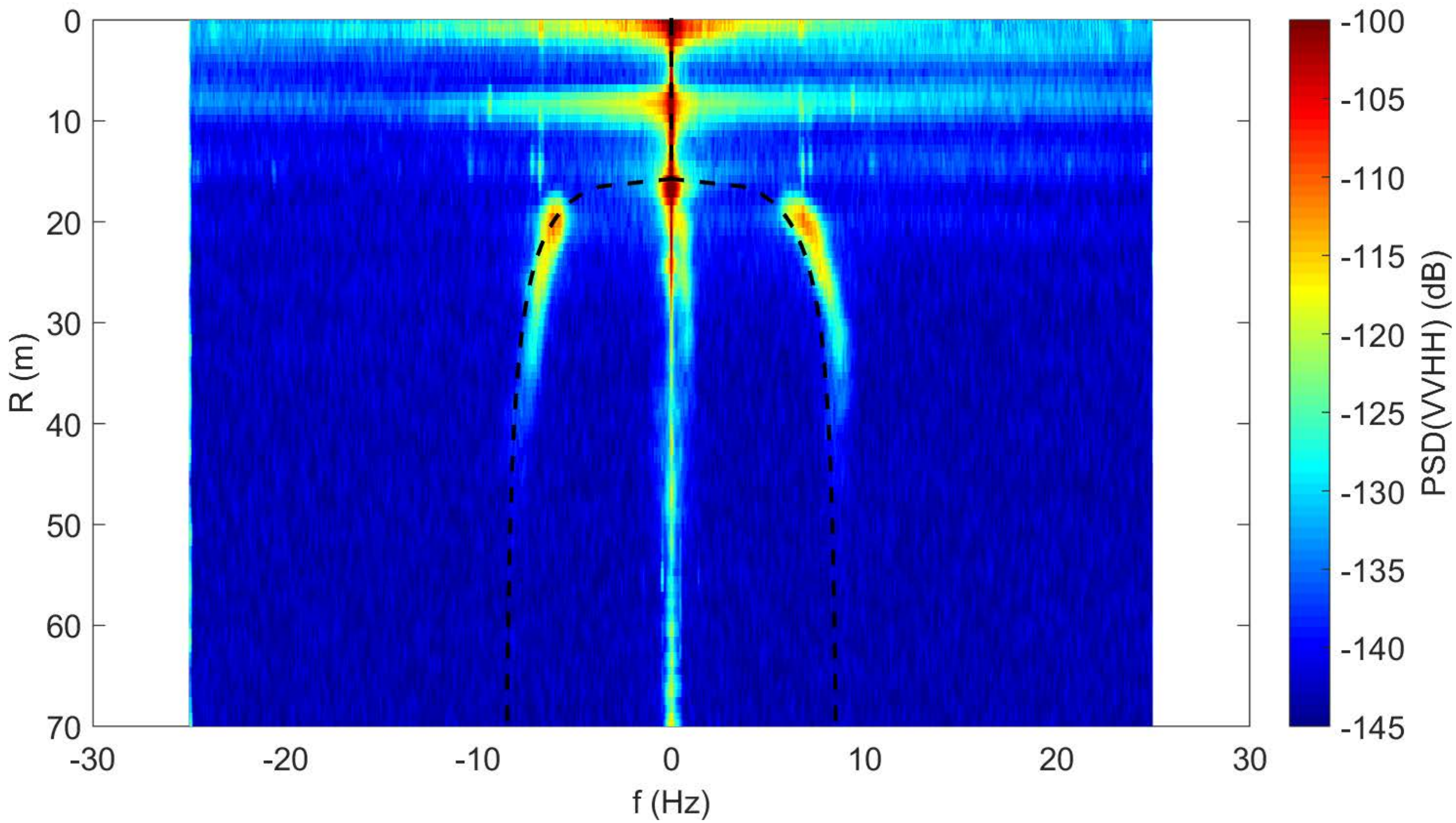

Doppler spectrum of radar return collects along the dispersion curves for gravity-capillary waves at the Bragg wavelength.

-> Seems to require very, very calm weather…

Instrument onboard the JCR (2)

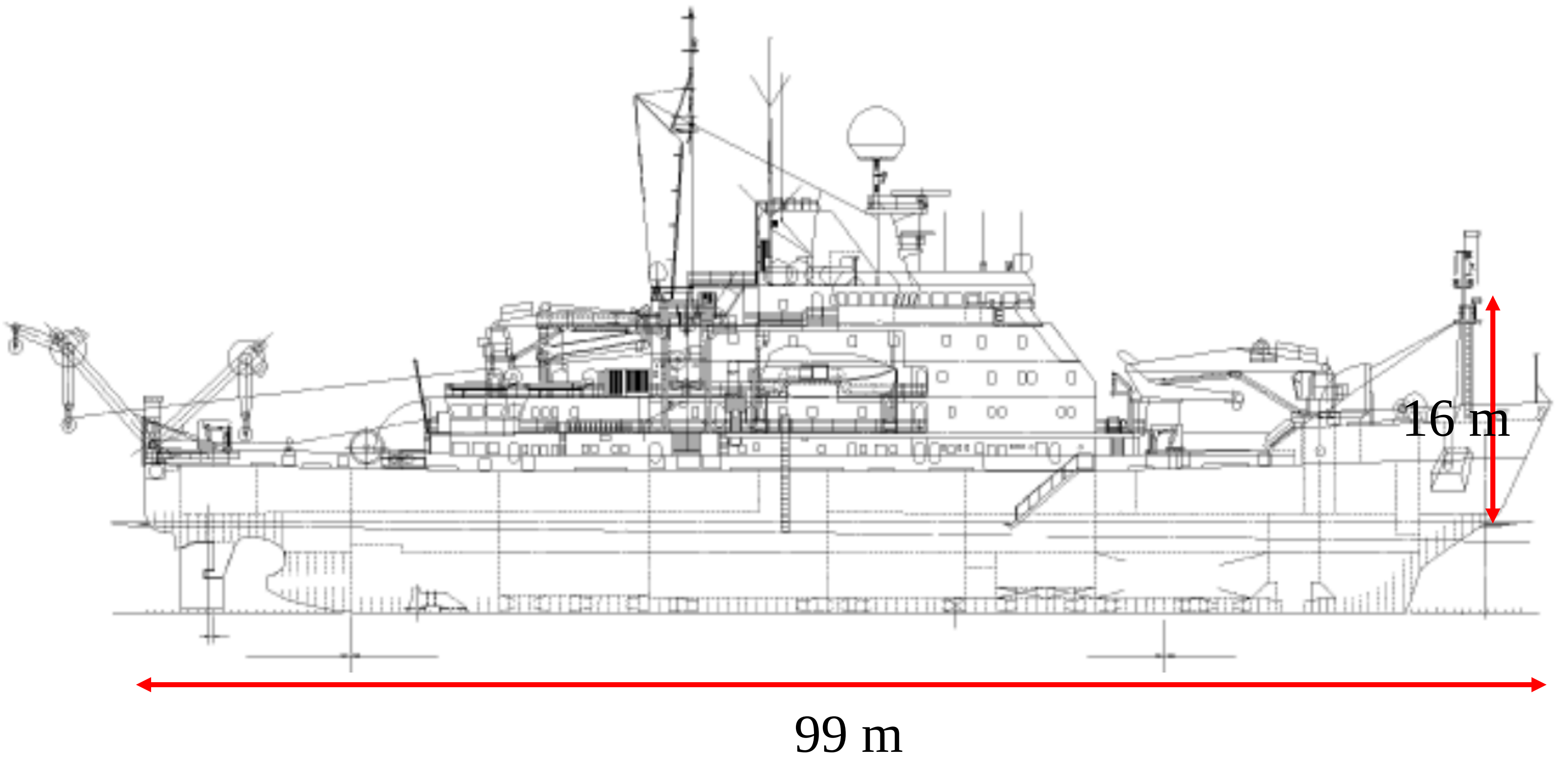

Instrument onboard the JCR (3)